

MICROMECHANICS MODELLING OF COMPRESSION MOLDED PA6/CARBON FIBRE LFT-D

Bondy, M^{1*}, Altenhof, W¹

¹ Mechanical, Automotive, and Materials Engineering,
University of Windsor, Ontario, Canada

* Corresponding author (bondy1z@uwindsor.ca)

Keywords: *LFT-D, carbon fibre, micromechanics modelling*

Abstract

Twelve combinations of micromechanics models and closure approximations were evaluated with respect to data from mechanical characterization for experimental fibre orientation and length distributions. Fibre orientation and length were also numerically estimated from mechanical data. The most accurate microstructure property estimates from this inverse process, in terms of prediction of mechanical properties, were obtained with the orthotropic fitted closure, a Weibull FLD, and the Mori-Tanaka micromechanics model (5.5% error). The quadratic closure combined with the Mori-Tanaka model performed very poorly for microstructure prediction, though allowing further iterations in the optimization process may improve these results. The FLD identified from mechanical properties was employed in a model of the error due to edge effects in obtaining this distribution experimentally. The experimental length distribution was not well approximated by the numerically identified FLD with modelling of edge effects.

1 Introduction

In the automotive industry, one of the most viable solutions for increasingly stringent fuel economy standards may be decreasing vehicle structural mass through the use of novel materials. Vehicle mass increased approximately 17% from 2000 to 2010 [1]. Fibre reinforced polymer (FRP) materials are optimal alternatives to structural metals in terms of specific stiffness and strength. However, thermosetting matrix materials, commonly used with continuous fibre where matrix viscosity must be low for fibre wetout, present challenges for minimum recyclability and recoverability in the European Union (85% and 95% of the vehicle, respectively). Compression molded, direct compounded long fibre thermoplastic (LFT-D) with carbon fibre (CF) combines recyclability with high performance mechanical characteristics.

2 Literature Review

Long fibre thermoplastics (LFTs) contain fibres with an average aspect ratio greater than 100 (approximate fibre length of 1-2 mm) [2, 3]. These materials have a number of advantages over other FRPs. Several mass production systems exist and have been in use in the automotive industry for many years [4]. One variation, LFT-D with inline compounding (ILC), can yield fibre lengths approximately an order of magnitude larger than from pellets. Tensile strength and fatigue characteristics are lower than a similar continuous fibre material but technologies exist for automated addition of localized continuous fibre reinforcement to discontinuous fibre parts [5]. Direct compounding also permits the use of any polymer/fibre/additive combination in any proportion permitted by the fibre orientation state in the compounding extruder. However, this flexibility in terms of material formulation requires personnel with the necessary expertise.

Few publications document mechanical properties of direct or in-line compounded materials. McLeod et al. [6] compared direct compounded injection and compression molded glass fibre/polypropylene. Significantly longer fibres were observed in the compression molding charge with respect to locations within the molded part and the nozzle of the injection molding machine where fibre length was significantly degraded. Poorer fibre

dispersion was noted for compression molded material with fibre rich/depleted zones. Flexural modulus was similar for compression and injection molded specimens. However, flexural yield strength was significantly higher for specimens extracted from compression molded parts.

Modelling of long fibre thermoplastics shares many similarities with the modelling process for short fibre materials. Local fibre orientation is described with the orientation tensor proposed by Tucker et al. [7]. Note that the fibre orientation distribution can be expected to vary in every direction including through the thickness. Commercial process modelling software is often limited to output of the 2nd order tensor. However, modelling of flow induced alignment and orientation averaging [8] to obtain mechanical characteristics by weighted averaging of unidirectional mechanical characteristics require the 4th order orientation tensor. A number of closure approximations exist to estimate the 4th order tensor from the 2nd order tensor including linear, quadratic, hybrid [7], natural [9], and orthotropic closures [10]. A number of micromechanics models exist for unidirectional fibre composite elasticity including: rule of mixtures (and its inverse), the Halpin-Tsai equations [11], the generalized self-consistent (GSC) model, and the Mori-Tanaka model [7]. The latter three were developed using the Eshelby method [8] for generating the stiffness tensor of an inclusion in a matrix.

A number of publications exist for limited experimental characterization and modelling of LFT materials. Garesci and Fliegner [9] reviewed the state of the art for this modelling process for the elastic response and validated their results with a limited number of non-destructive tensile tests. This study used μ CT data to obtain the fibre orientation distribution (in the form of the 2nd and 4th order tensors). Planar fibre and a symmetric orientation distribution were assumed. The fibre length distribution was obtained through image analysis after matrix burnoff. The Halpin-Tsai equations were employed to obtain the stiffness tensor for a unidirectional material. Nguyen et al. [8] documented their efforts to model the elastic properties of polypropylene with glass fibre for specimens extracted from two geometries: a centre gated disk and a rectangular ISO plaque. A process modelling code developed at the University of Illinois Urbana-Champaign, ORIENT, was used to model the fibre orientation distribution as a function of flow within the mold and was validated with optical microscopy. Readers interested in ORIENT can refer to [12]. The authors note the importance of high quality fibre orientation and length data for accurate model development.

Buck et al. [13] studied compression molded PP/GF with direct/in-line compounding. Fibre orientation was numerically predicted with Autodesk Moldflow® [14] and validated with μ CT data. Finite element structural models of dynamic mechanical analysis in the form of three point bending tests were developed and compared with experimental results. The authors employed the generalized self-consistent (GSC) micromechanics model which does not allow for including the influence of fibre length on elastic properties. Consequently, no data on the fibre length distribution was presented. Structural finite element models agree well with experiments in the flow region in the 0° direction (axis of loading aligned with flow direction). Accuracy for models of specimens loaded in the 45° and 90° directions is limited. In the charge region, models did not accurately predict material characteristics with percent error as high as 47%. However, fibre orientation within/between charges/plastificates (also referred to as unfinished product) may not be sufficiently repeatable to allow for accurate predictions of mechanical properties in this region.

3 Methodology

3.1 Mechanical & Microstructure Characterization

Polyamide 6 (BASF HS8202) and carbon fibre (Toho Tenax HTR40 F22 1550tex, 24k tow count) LFT was prepared on a Deiffenbacher LFT-D line at the Fraunhofer Project Centre in London, Ontario. Select details for the process configuration are provided in Table 1. For more details on the process and process parameters refer to [15]. Destructive uniaxial tensile tests and non-destructive three point bending tests were completed for dried and room temperature conditioned (30% relative humidity) specimens with orientations of 0°, +45°, -45°, and

90°. The fibre orientation distribution was measured for process configuration V2 by computed tomography with post-processing in MATLAB® and the open source software Compositight [16]. Fibre length distribution was measured by an industrial partner. Details on moisture absorption, conditioning, and procedures/apparatus for mechanical and microstructure characterization can be found in [15].

	V1	V2	V3	V4	V5	V6	V7	V8
Fibre weight fraction	12%	12%	12%	18%	18%	9%	9%	25%

Table 1: Process Configurations

3.2 Micromechanics Modelling

Halpin-Tsai, and Mori-Tanaka micromechanics equations were implemented in MATLAB® with linear, quadratic, hybrid, and orthotropic closure approximations. The fibre length distribution was incorporated for models employing the Halpin-Tsai and Mori-Tanaka micromechanics models. Mechanical properties for the constituent materials are given in Table 2. All models initially included fibre orientation data acquired by micro-computed tomography. Digimat® was also used both as a concomitant method and to employ more advanced models which include the mechanical anisotropy of the fibre (i.e. lower elastic modulus in the transverse direction). The Mori-Tanaka micromechanics model is available in Digimat but the Halpin Tsai model is not implemented. The MATLAB code is available at mathworks.com/matlabcentral/fileexchange/58020. Though it is currently under development, this MATLAB code includes the capability to map fibre orientation from an Autodesk Moldflow compression molding model to an LS-DYNA structural finite element model by creating a unique anisotropic material model for each element. Interpolating/extrapolating and mapping of multiple experimental fibre orientation measurements is also possible. Neither of these mapping options were employed in the current study.

Mechanical Property	Value	Mechanical Property	Value
Elastic modulus of PA6 (dried)	2.70 GPa [17]	Elastic modulus of carbon fibre (transverse)	15 GPa [18]
Elastic modulus of PA6 (conditioned)	2.50 GPa	In-plane Poisson’s ratio of carbon fibre	0.2 [18]
Poisson’s ratio of PA6	0.39 [19]	Transverse Poisson’s ratio of carbon fibre	0.25 [20]
Density of PA6	1.13 g/cc [17]	Transverse shear modulus of carbon fibre	5.25 GPa [20]
Elastic modulus of carbon fibre (longitudinal)	240 GPa [21]	Density of carbon fibre	1.81 g/cc [21]

Table 2: Mechanical properties of the fibre and matrix for micromechanics calculations

4 Results and Discussion

4.1 Mechanical and Microstructure Characterization

A large data set of mechanical and microstructure properties was collected and published in [15]. Only select results from microstructure characterization are included in this section. Experimental mechanical properties are included in the micromechanics modelling results. 2nd order orientation tensors (from Compositight and VG Studio) for a specimen extracted in close proximity to the specimens for mechanical characterization are given in Table 3. The Compositight orientation tensor was used for initial micromechanics modelling of tensile characteristics. More than one specimen was characterized by μ CT for fibre orientation but only one yielding acceptable orientation data was in close proximity to the mechanical characterization specimens. These were the first carbon fibre LFT specimens characterized by this research group. The small diameter of carbon fibres requires a small specimen for sufficient resolution. Another specimen in close proximity to the mechanical

characterization specimens was of a different, larger geometry. For more details on the fibre orientation characterization methodology, including specimen geometry and location, see [15].

Orientation tensor component	VG Studio	Composit/MATLAB
a_{11}	0.6487	0.6295
a_{12}	0.037	0.0281
a_{13}	-0.001	0.0187
a_{22}	0.3058	0.3134
a_{23}	0.0087	0.0078
a_{33}	0.0456	0.0570

Table 3: 2nd order orientation tensor

Two 100 mm by 100 mm sections of the 458 mm by 458 mm compression molded panels were sent to each of two industrial partners for fibre length characterization. One specimen was extracted from a panel with the lowest fibre weight fraction (process configuration V6, 9%) and the other was extracted from a panel with the highest weight fraction (process configuration V8, 25%). The industrial partners did not have extensive experience with direct compounding, though few laboratories have such expertise. One partner provided fibre length distribution data but noted that the longest fibres were entangled such that they could not be separated. The longest fibres were therefore discarded prior to any measurements of fibre lengths. The other partner was also dissatisfied with their efforts to separate the fibres and did not proceed to measuring fibre length. The fibre length distribution for process configuration V6 is shown in Figure 1. For process configuration V6, the number averaged and weight averaged fibre lengths are 327 and 584 microns respectively. Since the fibre diameter is approximately 7 microns, the average fibre aspect ratio is less than expected for an LFT material (~100). For more details and data on experimental characterization of fibre length see [15].

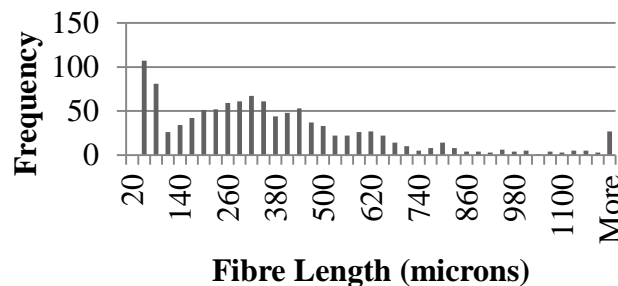


Figure 1: Fibre length distribution for process configuration V6 (9%)

4.2 Micromechanics Modelling

Comparisons of the elastic modulus in the 0° and 90° directions for the Halpin-Tsai and Mori-Tanaka micromechanics models and the linear, quadratic, hybrid, and orthotropic closure approximations are given in Table 4. The 4th order orientation tensor was also computed in MATLAB from μ CT data and input directly. For micromechanics modelling of 9% and 12% weight fractions, the experimental FLD from 9% material was input. For 18% and 25% weight fractions, FLD data for 25% was employed. The Halpin-Tsai model requires a maximum fibre volume fraction. This was defined to be 30% based upon values in the literature for maximum fibre volume fraction with a random in-plane fibre orientation state [20] – a similar fibre orientation state may exist in the fibre/polymer compounding extruder during processing, in the compression molding charge, and/or in the charge region of the compression molded plaque. Linear and hybrid closure approximations employed constants for in-plane fibre orientation states.

	Weight Fraction: 9%				Weight Fraction: 12%				Weight Fraction: 18%				Weight Fraction: 25%			
	Halpin-Tsai		Mori-Tanaka		Halpin-Tsai		Mori-Tanaka		Halpin-Tsai		Mori-Tanaka		Halpin-Tsai		Mori-Tanaka	
	0°	90°	0°	90°	0°	90°	0°	90°	0°	90°	0°	90°	0°	90°	0°	90°
Experiment [MPa]	8063	3771	8063	3771	9834	3784	9834	3784	14358	4846	14358	4846	20793	5711	20793	5711
CoV	5.1%	6.6%	5.1%	6.6%	4.7%	8.7%	4.7%	8.7%	6.6%	3.9%	6.6%	3.9%	6.3%	12.0%	6.3%	12.0%
a ₂ & a ₄	-21.9%	12.5%	-8.3%	22.3%	-21.2%	30.0%	-7.1%	41.4%	-31.4%	24.3%	-21.5%	30.2%	-30.5%	47.2%	-26.7%	40.6%
a ₂ & linear closure	-28.8%	7.2%	-18.5%	14.2%	-29.4%	22.2%	-19.5%	29.3%	-39.1%	16.4%	-33.6%	16.9%	-39.2%	37.4%	-41.2%	21.4%
a ₂ & quadratic closure	-45.2%	-23.7%	-41.1%	-25.9%	-48.2%	-19.0%	-45.0%	-23.2%	-56.4%	-26.2%	-56.4%	-35.2%	-57.8%	-18.0%	-63.3%	-39.3%
a ₂ & hybrid closure	-28.8%	7.2%	-18.5%	14.2%	-29.4%	22.2%	-19.5%	29.3%	-39.1%	16.4%	-33.6%	16.9%	-39.2%	37.4%	-41.2%	21.4%
a ₂ & orthotropic smooth closure	-15.5%	22.7%	0.2%	35.7%	-14.1%	43.6%	2.2%	59.3%	-25.0%	38.2%	-13.2%	48.2%	-23.9%	64.9%	-18.5%	62.3%
a ₂ & orthotropic fitted closure	-22.0%	12.2%	-8.5%	21.8%	-21.3%	29.5%	-7.3%	40.7%	-31.5%	23.9%	-21.6%	29.5%	-30.6%	46.7%	-26.8%	39.6%
a ₂ & ORW closure	-21.3%	13.2%	-7.6%	23.2%	-20.6%	30.9%	-6.3%	42.6%	-30.8%	25.3%	-20.7%	31.4%	-30.0%	48.5%	-25.9%	42.0%
Digmat-MF isotropic fibre	N/A	N/A	-10.2%	8.5%	N/A	N/A	-9.5%	23.0%	N/A	N/A	-19.6%	15.3%	N/A	N/A	-25.4%	22.2%
Digmat-MF orthotropic fibre	N/A	N/A	-10.9%	6.7%	N/A	N/A	-10.3%	20.6%	N/A	N/A	-20.5%	12.1%	N/A	N/A	-26.5%	17.9%

Table 4: Percent error for each micromechanics model and closure approximation for 0° and 90° elastic modulus; uncorrected experimental FLD, FOD from μ CT

When employing experimental FOD and FLD data, accuracy for the 90° direction was generally poor with stiffness over-estimated. As was observed in the analysis of the influence of fibre length that follows, use of experimental data for the fibre length distribution would not be expected to improve the accuracy since shorter fibres would reduce the 0° modulus. However, a coupling between fibre length and orientation could exist. The modelling tools developed for this study do not currently include such capabilities. In the 0° and 90° directions, the Halpin Tsai and Mori-Tanaka micromechanics models were similar in terms of accuracy (~25% error). The Halpin-Tsai model was more accurate for the -45° and 45° directions. For the 0° and 90° directions, direct computation of the 4th order tensor was similar in terms of accuracy to the 2D linear, 2D hybrid, orthotropic fitted, and ORW closure approximations. Percent error (absolute value) for each micromechanics model and closure approximation (for each direction) are shown in Table 5. Full results (i.e. the data in Table 4 for 0° and 90°) for +45° and -45° are not shown for brevity but will be presented.

It is unlikely that it is valid to use a fibre orientation distribution from one specimen from one process configuration. Numerous researchers have noted an influence of specimen geometry on mechanical properties since the longest fibres are approximately the same length as the width of the specimen gage region [15, 22, 23]. With direct compounding, poor fibre dispersion has also been observed as noted in the literature review. A CT specimen sufficiently small to allow for the precision required for carbon fibres may not accurately capture the orientation distribution associated with both well and poorly dispersed fibres. Therefore, a numerical approach was employed to use experimental mechanical properties to find the 2nd order orientation tensor for each process configuration. Table 6 includes the 2nd order orientation tensors identified numerically from mechanical properties for 12% fibre weight fraction. The 1st two rows are the experimental data previously given in Table 3. Note that there is no dependence on micromechanics model for these first two rows and the same tensor is given for both micromechanics models for ease of comparison. Table 7 is a summary of the accuracy of each micromechanics model and closure approximation after completing this optimization process.

	Halpin Tsai					Mori-Tanaka				
	-45°	0°	45°	90°	Mean	-45°	0°	45°	90°	Mean
a₂ & a₄	14.1%	26.2%	10.0%	28.5%	19.7%	21.6%	15.9%	11.1%	33.6%	20.6%
a₂ & linear	12.6%	34.1%	10.3%	20.8%	19.4%	13.7%	28.2%	6.2%	20.4%	17.1%
a₂ & quadratic	34.5%	51.9%	39.8%	21.7%	37.0%	41.3%	51.4%	45.3%	30.9%	42.2%
a₂ & hybrid	12.6%	34.1%	10.3%	20.8%	19.4%	13.7%	28.2%	6.2%	20.4%	17.1%
a₂ & orthotropic smooth	10.4%	19.6%	12.2%	42.4%	21.2%	11.8%	9.5%	6.0%	51.4%	19.7%
a₂ & orthotropic fitted	13.5%	26.4%	10.1%	28.1%	19.5%	19.8%	16.1%	11.0%	32.9%	20.0%
a₂ & ORW	13.6%	25.7%	10.0%	29.5%	19.7%	20.2%	15.1%	11.2%	34.8%	20.3%
Digmat (a₂ & hybrid, isotropic fibre)	N/A	N/A	N/A	N/A	N/A	42.8%	16.2%	39.9%	17.3%	29.0%
Digmat (a₂ & hybrid, transversely orthotropic fibre)	N/A	N/A	N/A	N/A	N/A	40.6%	17.1%	38.3%	14.4%	27.6%

Table 5: Summary of micromechanics model and closure approximation accuracy for all fibre weight fractions; uncorrected experimental FLD, FOD from μ CT

Closure Approximation	Halpin Tsai					Mori-Tanaka				
	a ₁₁	a ₂₂	a ₁₂	a ₁₃	a ₂₃	a ₁₁	a ₂₂	a ₁₂	a ₁₃	a ₂₃
μCT (VG Studio)	0.6487	0.3058	0.0281	-0.001	0.0087	0.6487	0.3058	0.0281	-0.001	0.0087
μCT (Composight & MATLAB)	0.6295	0.3137	0.0281	0.0187	0.0078	0.6295	0.3137	0.0281	0.0187	0.0078
Linear	0.7281	0.2038	0.03252	0.0201	0.00816	0.7182	0.2246	0.1094	0.1048	-0.0332
Quadratic	0.7000	0.2128	0.01454	0.0129	0.00144	0.7884	0.2117	0.0255	0.0163	0.00833
Hybrid	0.7840	0.1507	0.02248	0.0162	0.00810	0.7623	0.1813	0.03223	0.0251	0.00777
Orthotropic smooth	0.6384	0.2728	0.04472	0.0101	0.005635	0.6123	0.1939	0.03621	0.03374	0.004059
Orthotropic fitted	0.7068	0.2153	0.0338	0.01868	0.007964	0.7010	0.2254	0.02983	0.018335	0.01112
ORW	0.7003	0.2207	0.02973	0.01982	0.008685	0.6975	0.2292	0.01916	0.00999	0.01249

Table 6: 2nd order orientation tensors from optimization for 12% fibre weight content

A small number of the 2nd order orientation tensors identified through this numerical inverse microstructure characterization process are suspect since they describe a fibre orientation state that cannot be approximated as planar and the specimens are extracted from a thin (~ 3 mm) panel. The constant fibre aspect ratio was simultaneously optimized for each micromechanics model and closure approximation (average aspect ratio was 97 but the coefficient of variation was 58%). For a number of closure approximation/micromechanics model combinations, the optimization methodology failed to converge to a solution meeting the defined criteria. The number of iterations was increased from 1200 to 10000 without any significant influence on the results.

	Halpin Tsai					Mori-Tanaka				
	-45°	0°	45°	90°	Mean	-45°	0°	45°	90°	Mean
a₂ & linear	7.7%	39.8%	14.5%	6.1%	17.0%	6.7%	31.9%	6.1%	3.7%	12.1%
a₂ & quadratic	7.2%	17.8%	9.8%	19.5%	13.6%	42.0%	23.6%	48.1%	30.5%	36.0%
a₂ & hybrid	8.6%	31.8%	15.7%	9.4%	16.4%	10.1%	28.1%	12.7%	13.4%	16.1%
a₂ & orthotropic smooth	15.4%	25.6%	22.0%	15.2%	19.6%	21.7%	17.6%	25.8%	9.4%	18.6%
a₂ & orthotropic fitted	12.3%	24.7%	17.6%	3.7%	14.6%	10.5%	11.0%	10.7%	6.8%	9.8%
a₂ & ORW	10.7%	24.6%	19.2%	3.6%	14.5%	7.2%	13.2%	12.7%	4.2%	9.3%

Table 7: Summary of micromechanics model and closure approximation accuracy for all fibre weight fractions; FOD and average fibre length from numerical optimization

Further inverse microstructure characterization was completed with a Weibull fibre length distribution where the initial estimates for the Weibull parameters were maximum likelihood estimates for the experimental FLD data sets from the industrial partner. The resulting Weibull distributions were then used as an input to a MATLAB model which randomly positions and orientates fibre within a 100 mm by 100 mm region (the size of the specimen provided to the industrial partner). To the best of the authors' knowledge, the industrial partner reduced this specimen to 20 mm by 20 mm and did not correct for 'edge effects' (artificially short fibres introduced by cutting the specimen). Procedures for experimentally eliminating edge effects and removing any such bias are well documented in the open literature [24] but are not standard practice in the laboratory of the industrial partner. The MATLAB code developed identifies any fibres within or intersecting the 20 mm by 20 mm subregion and extracts the fibre lengths for fibres entirely within or cut by the perimeter of this subregion. As shown in Figure 2, the FLD is affected by edge effects, even for a specimen that is much larger than the longest fibres. However, this modelling of edge effects, starting with an FLD identified from optimized mechanical properties, does not yield an FLD, including edge effects, similar to the experimental FLD from the industrial partner. The methodology employed for modelling edge effects is computationally expensive but an ideal approach would be to incorporate this edge effects model into the process of identifying the FLD from mechanical properties. This improved FLD from mechanical properties would be optimized to both yield accurate mechanical responses and agree with the experimental observations of fibre length.

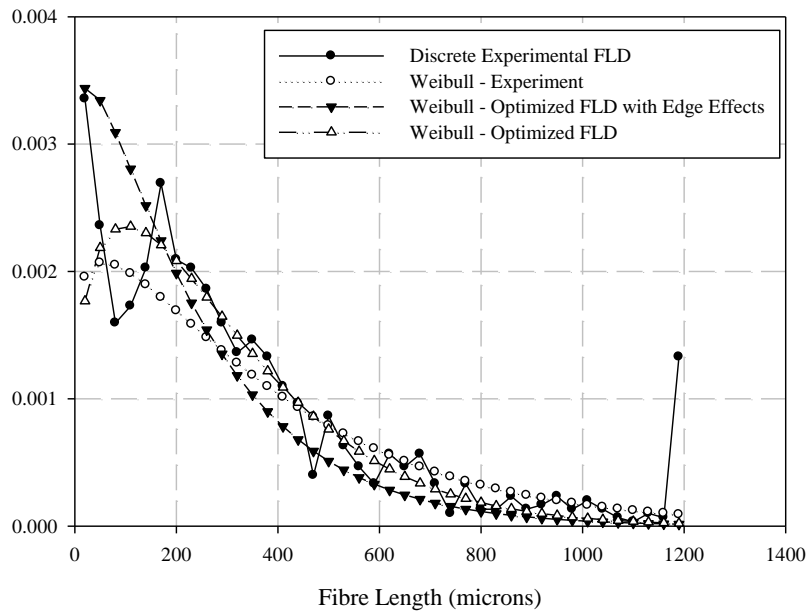


Figure 2: Fibre Length Distribution Modelling

Fibre Weight Content	Halpin Tsai					Mori-Tanaka				
	a_{11}	a_{22}	a_{12}	a_{13}	a_{23}	a_{11}	a_{22}	a_{12}	a_{13}	a_{23}
9%	0.7086	0.2304	0.0402	0.0201	0.0072	0.7051	0.2369	0.0276	0.0205	0.0086
12%	0.7065	0.2159	0.0399	0.0168	0.0082	0.7102	0.2202	0.0825	-0.007	0.0068
18%	0.7379	0.2015	0.0282	0.0220	0.0087	0.7312	0.2106	0.1094	0.0114	-0.064
25%	0.8144	0.1315	0.0275	0.0191	0.0084	0.7883	0.1699	-0.002	0.0120	0.0120

Table 8: Fibre orientation as a function of fibre weight fraction

The orthotropic fitted closure yielded the most accurate elastic moduli when a Weibull FLD was assumed, as shown in Table 9. The orientation tensors for this closure approximation are presented as a function of fibre weight fraction in Table 8. Increased alignment of fibre in the flow direction occurs resulting in a more anisotropic material as fibre content increases. This change in average through thickness FOD may be associated with a change in the through thickness structure (i.e. skin/core). Flexural properties suggest that such a change in through thickness FOD with increasing fibre content may occur [15]. One of the next steps in this research will be to employ laminate theory to investigate this phenomenon.

	Halpin Tsai					Mori-Tanaka				
	-45°	0°	45°	90°	Mean	-45°	0°	45°	90°	Mean
a₂ & linear	10.1%	28.3%	6.7%	1.9%	11.8%	7.6%	26.7%	3.8%	2.5%	10.1%
a₂ & quadratic	35.0%	1.6%	40.8%	20.8%	24.6%	40.1%	1.6%	45.7%	30.3%	29.4%
a₂ & hybrid	5.9%	8.4%	2.5%	9.8%	6.6%	7.1%	10.1%	2.9%	10.1%	7.6%
a₂ & orthotropic smooth	7.7%	1.6%	6.1%	35.7%	12.8%	10.4%	1.6%	8.4%	25.9%	11.6%
a₂ & orthotropic fitted	6.5%	1.6%	3.5%	12.3%	6.0%	8.6%	2.1%	5.0%	6.2%	5.5%
a₂ & ORW	6.5%	1.6%	3.6%	14.8%	6.6%	6.7%	1.6%	4.1%	12.2%	6.2%

Table 9: Summary of micromechanics model and closure approximation accuracy for all fibre weight fractions; FOD and FLD from numerical optimization

5 Conclusions and Future Work

Twelve combinations of micromechanics models and closure approximations were evaluated with respect to data from mechanical characterization for experimental fibre orientation and length distributions. Fibre orientation and length were also numerically estimated from mechanical data. The most accurate microstructure property estimates from this inverse process, in terms of prediction of mechanical properties, were obtained with the orthotropic fitted closure, a Weibull FLD, and the Mori-Tanaka micromechanics model (5.5% error). The quadratic closure combined with the Mori-Tanaka model performed very poorly for microstructure prediction, though allowing further iterations in the optimization process may improve these results. The FLD identified from mechanical properties was employed in a model of the error due to edge effects in obtaining this distribution experimentally. The experimental length distribution was not well approximated by the numerically identified FLD with modelling of edge effects. If the modelling of fibre edge effects can be completed with greater computational efficiency, an inverse process to quantify the microstructure could be developed to both predict mechanical properties and a fibre length distribution consistent with experimental observations. Additionally, there remain questions regarding a possible change in fibre orientation through the part thickness. The application of laminate theory would permit a numerical investigation of this topic.

6 References

- [1] L. Chauvet, *Trelleborg Weight Reduction Strategy-Utilization of Plastic for Structural Components for Power Train Mounting System*. 2012, SAE Technical Paper # 2012-28-0017.
- [2] J. Thomason, The influence of fibre length and concentration on the properties of glass fibre reinforced polypropylene: 5. Injection moulded long and short fibre PP. *Composites Part A: Applied Science and Manufacturing*, 2002. 33(12): p. 1641-1652.
- [3] M. Schemme, LFT—development status and perspectives. *Reinforced Plastics*, 2008. 52(1): p. 32-39.
- [4] W. Krause, F. Henning, S. Tröster, O. Geiger, and P. Eyerer, LFT-D—a process technology for large scale production of fiber reinforced thermoplastic components. *Journal of Thermoplastic Composite Materials*, 2003. 16(4): p. 289-302.
- [5] M. Brümmer, F. Henning, and W. Krause, Long-Fiber Reinforced Thermoplastics Tailored for Structural Performance. *SPE ACCE*, 2005.
- [6] M. McLeod, E. Baril, J. Hetu, T. Deaville, and M. Bureau. *Morphological and Mechanical Comparison of Injection and Compression Moulding In-Line Compounding of Direct Long Fibre Thermoplastics*. in *SPE Automotive Composites*. 2010. Troy, MI: SPE.

- [7] S. Advani and C. Tucker, The use of tensors to describe and predict fiber orientation in short fiber composites. *Journal of Rheology (1978-present)*, 1987. 31(8): p. 751-784.
- [8] B. Nguyen, S. Bapanapalli, J. Holbery, M. Smith, V. Kunc, B. Frame, J. Phelps, and C. Tucker, Fiber length and orientation in long-fiber injection-molded thermoplastics—Part I: Modeling of microstructure and elastic properties. *Journal of Composite Materials*, 2008. 42(10): p. 1003-1029.
- [9] V. Verleye, A. Coumiot, and F. Dupret. *Prediction of fiber orientation in complex injection molded parts*. in *ICCM/9*. 1993.
- [10] J.S. Cintra Jr and C.L. Tucker III, Orthotropic closure approximations for flow-induced fiber orientation. *Journal of Rheology (1978-present)*, 1995. 39(6): p. 1095-1122.
- [11] J. Halpin and J. Kardos, The Halpin-Tsai equations: a review. *Polymer Engineering & Science*, 1976. 16(5): p. 344-352.
- [12] R.S. Bay and C.L. Tucker, Fiber orientation in simple injection moldings. Part I: Theory and numerical methods. *Polymer composites*, 1992. 13(4): p. 317-331.
- [13] F. Buck, B. Brylka, V. Müller, T. Müller, A.N. Hrymak, F. Henning, and T. Böhlke. *Coupling of mold flow simulations with two-scale structural mechanical simulations for long fiber reinforced thermoplastics*. in *Materials Science Forum*. 2015. Trans Tech Publ.
- [14] Autodesk Moldflow. 2017, Autodesk.
- [15] M. Bondy, P. Pinter, and W. Altenhof, Experimental characterization and modelling of the elastic properties of direct compounded compression molded carbon fibre/polyamide 6 long fibre thermoplastic. *Materials & Design*, 2017.
- [16] B. Bertram and P. Pinter, *Composight*. 2016, Sourceforge.
- [17] BASF. *Product Information: Ultramid 8202 HS Polyamide 6*. [09/16/2016]; Available from: <http://www.plasticsportal.com/products/dspdf.php?type=iso¶m=Ultramid+8202+HS>.
- [18] R.F. Gibson, *Principles of composite material mechanics*. Vol. 218. 2012: CRC press.
- [19] Professional Plastics. *Mechanical Properties of Plastic Materials*. [09/16/2016]; Available from: <http://www.professionalplastics.com/professionalplastics/MechanicalPropertiesofPlastics.pdf>.
- [20] K. Evans and A. Gibson, Prediction of the maximum packing fraction achievable in randomly oriented short-fibre composites. *Composites science and technology*, 1986. 25(2): p. 149-162.
- [21] Toho Tenax America, *Test Report - Tenax-A HTR40 F22 24K 1550TEX*. 2013. p. 1.
- [22] K. Rohan, T. McDonough, V. Ugresic, E. Potyra, and F. Henning, *Mechanical Study of Direct Long Fiber Thermoplastic Carbon/Polyamide 6 and its Relations to Processing Parameters*. 2015, University of Western Ontario/Zoltek Corporation. p. 1-24.
- [23] R. Marissen and J. Linsen, Variability of the flexural strength of sheet moulding compounds. *Composites Science and Technology*, 1999. 59(14): p. 2093-2100.
- [24] F.B. Kunc V, Nguyen BN, Tucker III CL, Velez-Garcia G *Fiber Length Distribution Measurement for Long Glass and Carbon Fiber Reinforced Injection Molded Thermoplastics*. in *7th Annual SPE Automotive Composites Conference and Exposition*. 2007. Troy, MI: Society of Plastics Engineers.